Bioorganic & Medicinal Chemistry 28 (2020) 115684

Contents lists available at ScienceDirect

Bioorganic & Medicinal Chemistry

journal homepage: www.elsevier.com/locate/bmc

# A 2-step synthesis of Combretastatin A-4 and derivatives as potent tubulin assembly inhibitors

Natalie G. Barnes[a,1], Anthony W. Parker[b], Amjed A. Ahmed Mal Ullah[a,2], Patricia A. Ragazzon[a,3], John A. Hadfield[a,*]

[a] Biomedical Research Centre, Kidscan Laboratories, School of Science, Engineering and Environment, University of Salford, Salford, UK
[b] Central Laser Facility, Research Complex at Harwell, Rutherford Appleton Laboratory, STFC, Chilton, Oxfordshire OX11 0QX, UK

ARTICLE INFO

*Keywords:*
Combretastatin A-4
Tubulin
Cancer
Microtubules

ABSTRACT

A series of combretastatin derivatives were designed and synthesised by a two-step stereoselective synthesis by use of Wittig olefination followed by Suzuki cross-coupling. Interestingly, all new compounds (2a-2i) showed potent cell-based antiproliferative activities in nanomolar concentrations. Among the compounds, 2a, 2b and 2e were the most active across three cancer cell lines. In addition, these compounds inhibited the polymerisation of tubulin *in vitro* more efficiently than CA-4. They caused cell cycle arrest in $G_2$/M phase further confirming their ability to inhibit tubulin polymerisation.

## 1. Introduction

Microtubules are critical for cellular functions such as mitosis and cell structure. Mitosis is a key stage of cell division in which chromosomes are separated producing genetically identical daughter cells; the mitotic spindle is the cytoskeletal structure of cells that forms to separate these daughter cells. Interference with microtubule formation hinders the formation of this mitotic spindle required for cell division leading to mitotic arrest and eventual apoptosis (cell death). A number of microtubule targeting agents have been clinically successful in the treatment of cancer, making microtubules a significant target for anticancer drugs.[1–4] Microtubule agents either inhibit or accelerate microtubule formation causing disruption to the formation of the mitotic spindle. A number of both natural and synthetic compounds target microtubule polymerisation with most of the antimitotic agents in use today being plant derivatives.[5–6] Taxoids bind to tubulin, stabilizing the microtubules by accelerating polymerisation. Taxol (or paclitaxel) is routinely used in the treatment of a number of cancers including ovarian, breast, lung and pancreatic cancer.[7] Vinca alkaloids and colchicine (1) induce depolymerisation of microtubules. Vinca alkaloids are used in clinical practice to treat solid tumours mainly of the lung, testicle and breast. A number of natural ligands bind to the colchicine binding site of tubulin including combretastatin A-4 (CA-4, 2),[8] and podophyllotoxin (3)[9] (Fig. 1). These agents comprise *cis*-locked aryl groups one of which is 3,4,5-trimethoxyphenyl.

Tumour vasculature is a known therapeutic target for cancer treatment. A number of preclinical *in vivo* investigations and clinical trials have evaluated the toxicity of vascular disrupting agents (VDAs).[10–12] However in several cases, VDAs have been shown to cause detrimental effects to the cardiovascular system due to long term dosing.[13] Recently, VDAs have been investigated to overcome these effects by employing a glutamic acid conjugate[14] and with VDA-induced aggregation of gold nanoparticles to furtjer destroy tumour vasculature.[15]

Combretastatins are a group of natural products isolated from the bark of the South African willow *Combretum caffrum*.[16] Combretastatins are of increasing interest due to their simple structures and easy synthesis.[17] The most active combretastatin known to date CA-4 (2) binds to the colchicine site of tubulin, disrupting microtubule polymerisation and eventually induces apoptosis.[18–20] CA-4 disrupts endothelial cell structure in tumour capillaries, limiting blood flow and causing cell death[21–23] and so can be classed as a VDA. CA-4 is a poorly water-soluble compound and so a number of water-soluble prodrugs have been developed including combretastatin A4 disodium phosphate (CA4-4P) which is converted into Z-CA4 by cellular phosphatases in the body.[24] Preclinical and clinical trials of the water soluble phosphate

* Corresponding author.
*E-mail address:* j.a.hadfield@salford.ac.uk (J.A. Hadfield).
[1] Present address: Department of Chemistry, University College London, London, UK.
[2] Permanent address: Chemistry Department, Science College, University of Basrah, Iraq.
[3] Present address: School of Pharmacy and Bioengineering, Keele University, Newcastle, UK.

https://doi.org/10.1016/j.bmc.2020.115684
Received 15 June 2020; Received in revised form 22 July 2020; Accepted 28 July 2020
Available online 05 August 2020

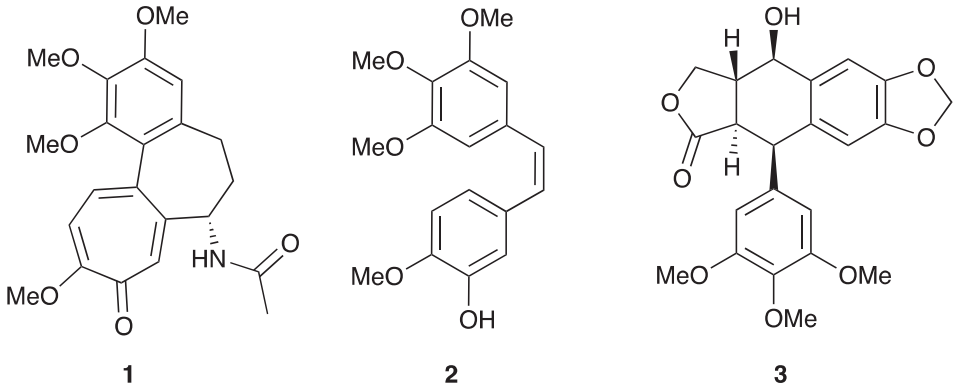


**Fig. 1.** Structure of natural ligands that bind at the colchicine site of tubulin.

prodrug CA4-P identified resistance at the tumour periphery;[22,25–29] to overcome this combretastatins have been investigated as a combination therapy to complement traditional anticancer approaches.[23,30–37] Limited advancement of these combination trials could be attributed to cardiovascular adverse events of CA4P.[38] More recently, combretastatin A-1 diphosphate (OXi4503) has been in clinical trials for patients with relapsed or refractory acute myeloid leukemia[39] or myelodysplastic syndromes.[40] Combretastatins are also being investigated for photodynamic therapy as a means to overcome the acute toxic effects of the *cis*-isomers and provide a more targeted treatment through photoactivated isomerisation of the non toxic *trans*-form.[41–42]

Combretastatins continue to be compounds of interest with an increasing number of structurally modified combretastatin derivatives synthesized to exploit their properties for targeted therapeutic applications as VDAs. Modifications of combretastatins tended to retain the more cytotoxic *cis*-conformation which included restriction of the *cis*-configuration by replacement of the olefinic bond with heterocyclic rings such as imidazole[43], pyrazole[44], triazole[45] etc. There are a number of studies involving both modification on the olefinic bond and aromatic rings of CA-4.[46–48] Modifications to the A-[49] and B-[50–51] rings have also been investigated to try and improve activity and solubility.

Synthetic routes for *cis*-stilbenes include the Wittig reaction,[52] alkyne hydroboration,[53] selective reduction of alkynes using a Lindlar catalyst,[54] Perkin condensation,[55] Kumada-Corriu cross-coupling[56], Negishi coupling[57] and Ramberg–Bäcklund reaction.[58] A very useful reaction for the stereoselective synthesis of *cis*-stilbenes is the Suzuki cross-coupling. The Suzuki cross-coupling reaction has a broad application in the formation of carbon-carbon bonds owing to the mild reaction conditions and broad functional group toleration.[59]

## 2. Results and discussion

### 2.1. Chemistry results

Our designed combretastatin derivatives possess a 3,4,5-trimethoxyphenyl A-ring and electron withdrawing groups at the 2- and 4-position of the B-ring (table 1). There are several syntheses of combretastatins in the literature.[52–59] Most of these methods failed to provide the required combretastatin derivatives, however a Suzuki cross coupling method proved successful.

The general synthetic route for combretastatin derivatives 2a-m is illustrated in Scheme 1. 3,4,5-Trimethoxy-β-iodostyrene (6) was readily prepared using Stork-Zhao olefination methodology[60] from iodomethylenetriphenylphosphonium iodide (4) (1.3 equivalents) and 3,4,5-trimethoxybenzaldehyde (5) in the presence of NaHMDS (1.3 equivalents) in 72% yield. *Z*-Combretastatins were synthesised following the Suzuki-coupling of this *Z*-iodostyrene compound with appropriately substituted aryl boronic acids (Scheme 1).

To further investigate the scope of this method and to extend the compound library, we synthesised 3-hydroxy substituted combretastatins. The boronic acids required for this synthesis were not commercially available. Although boronic acids react more efficiently, we chose to synthesise the corresponding boronic pinacol esters as they are easier to isolate and purify.[61] The boronic pinacol esters were synthesised by Miyaura borylation;[59] bis(pinacolato)diboron ($B_2pin_2$) was reacted with aryl halides in the presence of a palladium catalyst and potassium acetate. Z-Combretastatins were then synthesised as described above from 6 and appropriately substituted pinacol esters. We synthesised a small library of both known and unknown compounds with a variety of substituents including CHO (2a), CN (2h), $NO_2$ (2j, 2k) and 3,4,5-trimethoxy (2l) in order to show the broad functional group toleration of this method (Table 1). Novel synthesised compounds were characterised by $^1H$ and $^{13}C$ NMR as well as High Resolution Mass Spectrometry.

Application of this 2-step method to the synthesis of combretastatin A-4 gave an overall yield of 56% following purification by column chromatography and recrystallisation from methanol (Scheme 2). This was a huge improvement to the previously reported Suzuki cross-coupling synthesis. Gaukroger *et al* reported a 5-step process with an overall yield of 16%.[59] Further to this, we avoided the use of highly toxic carbon tetrabromide and tin. Malysheva and co-workers reported a 2-step synthesis of combretastatin derivatives by Negishi cross-coupling of **6** with overall yields of 25–45%.[57] Negishi coupling however requires phenol protection; they synthesised combretastatin A-4 in 39% overall yield. Our method provides a higher yielding synthesis of combretastatin derivatives without the need to protect functional groups.

### 2.2. Biological results

#### 2.2.1. Antiproliferative activities of compounds 2a-2i

We determined the cytotoxicity of these new analogues across three human cancer cell lines (table 1). The half-maximal inhibitory concentration ($IC_{50}$) for all new compounds (2a-2i) tested against HepG2 hepatic carcinoma, HCT-116 colon cancer and HeLa human epithelial cervical cancer cells is shown in Table 1. We chose cell lines previously used for CA-4;[62–65] CA-4 was used as a control to compare the potency of the synthesized combretastatin analogues.

As shown in Table 1 most of the combretastatin derivatives show antiproliferative activity in the micromolar range, although not as active as CA-4. The most active compounds were 2b (HeLa, HCT-116) and 2e (HepG2) with $IC_{50}$ values of less than 100 nanomolar.

Generally, the presence of an electron withdrawing carbonyl group in the 4-position of the B-ring provided potent anti-proliferative activities. Based on the binding determined for CA-4,[66] it can be presumed this is due to hydrophobic interactions in the colchicine binding site of tubulin at the 4-position of these derivatives. Further to this, compounds lacking a 4-substitution pattern (2d, 2g) or with a nitrile group

**Table 1**

Structures of synthesised compounds 2a-m and antiproliferative activities of compounds 2a-i against human cancer cell lines *in vitro*.

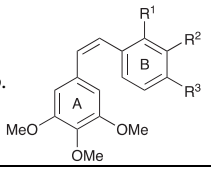


| Comp. | $R^1$ | $R^2$ | $R^3$ | *In vitro* cytotoxicity (IC50 ± SD, μM) | | |
|---|---|---|---|---|---|---|
| | | | | HepG2 | HeLa | HCT-116 |
| **2a** | H | H | CHO | 0.25 ± 0.05 | 0.28 ± 0.06 | 0.27 ± 0.15 |
| **2b** | H | OH | CHO | 0.23 ± 0.05 | 0.07 ± 0.01 | 0.09 ± 0.03 |
| **2c** | CHO | H | OMe | 0.14 ± 0.03 | 0.15 ± 0.03 | 0.14 ± 0.09 |
| **2d** | CHO | H | H | 1.06 ± 0.38 | 1.21 ± 0.31 | 2.61 ± 1.51 |
| **2e** | H | H | C(=O)Me | 0.06 ± 0.03 | 0.14 ± 0.02 | 0.25 ± 0.12 |
| **2f** | H | OH | C(=O)Me | 0.37 ± 0.09 | 0.34 ± 0.10 | 0.35 ± 0.23 |
| **2g** | C(=O)Me | H | H | 0.46 ± 0.12 | 0.14 ± 0.08 | 0.45 ± 0.12 |
| **2h** | H | H | CN | 0.96 ± 0.35 | 0.46 ± 0.10 | 1.42 ± 0.40 |
| **2i** | H | OH | CN | 0.53 ± 0.24 | 0.58 ± 0.13 | 0.79 ± 0.21 |
| **2j** | H | H | $NO_2$ | n.d | n.d | n.d |
| **2k** | $NO_2$ | H | H | n.d | n.d | n.d |
| **2l** | OMe | OMe | OMe | n.d | n.d | n.d |
| **2m** | H | H | H | n.d | n.d | n.d |
| **CA-4** | H | OH | OMe | 0.006 ± 0.001 | 0.007 ± 0.002 | 0.010 ± 0.003 |

$IC_{50}$ was determined after 72 h of drug exposure. Each experiment was carried out in triplicate at least two times. SD represents standard deviation.

(2h, 2i) showed limited cytotoxicity. 3-Hydroxy substitution was not essential for anti-proliferative activity but increased the activity when combined with a 4-carbonyl substitution (2b).

### 2.2.2. Effect on microtubules

CA-4 is a microtubule-destabilising agent that binds with tubulin at the same site as that of colchicine.[67–68] Combretastatins are known to depolymerize cellular microtubules. The inhibition of tubulin polymerisation by the combretastatin derivatives was tested using bovine brain tubulin.

We analyzed the effect of compounds 2a-2i on the assembly kinetics of tubulin *in vitro* using a fluorescence-based assay. Combretastatins 2a, 2b and 2e inhibited tubulin polymerisation almost completely at 1 μM (Fig. 2a); interestingly, these compounds were also the most cytotoxic. Compounds 2c, 2f and 2h slowed the rate of tubulin polymerisation with maximum polymerisation below that of untreated tubulin (Fig. 2b). These compounds showed a similar trend in cytotoxicity; they effected cell proliferation but were not as potent as 2a, 2b and 2e. Although compounds 2d, 2g and 2i didn't inhibit the final proportion of tubulin polymerised at a concentration of 1 μM (Fig. 2c), these compounds appeared to slow down the rate of tubulin polymerisation.

Compounds 2d and 2g displayed tubulin polymerisation curves comparable to that of untreated tubulin with a clear growth phase. The rate of tubulin polymerisation was estimated by fitting the early times of the curve to a pseudo-first order rate equation (Table 2). Values for compound 2i were not determined as the one–phase association was ambiguous. The rate constant (k) of microtubule formation under normal conditions was 0.0208 $min^{-1}$ with a half-life of 33 min. Incubation with compounds 2d and 2g decreased the rate of microtubule formation with k values of 0.0116 $min^{-1}$, 0.0123 $min^{-1}$ respectively. The half-life of tubulin formation also increased upon treatment with compounds 2d and 2g confirming that although the final volume of microtubules did not appear to be inhibited, these compounds slowed down the rate of tubulin polymerisation (k) and thus expected to disrupt the cell signalling pathways, as demonstrated by the cell toxicity results, Table 1.[17]

An $IC_{50}$ of the tubulin polymerisation was determined from the $V_{max}$ of the polymerisation curves at varying concentrations for 2a, 2b and 2e (Fig. 2d). These combretastatin derivatives had $IC_{50}$ values of 0.39, 0.32 and 0.28 μM respectively. This is almost a 10-fold increase in inhibition of tubulin polymerisation than that of colchicine (2.68 μM).[69] Further to this, CA-4 is reported as one of the most potent tubulin polymerisation inhibitors with $IC_{50}$ values reported to range from 0.53 to 2.4 μM.[69–72] The inhibition of tubulin polymerisation correlated with the cytotoxicity towards cancer cell lines suggesting the main mode of action of these combretastatin derivatives is the inhibition of tubulin polymerisation.[71–74]

### 2.2.3. Effect on cell cycle arrest

During mitosis, the microtubule is critical for the separation of chromosomes. Exposure to microtubule targeting agents leads to damaged mitotic spindles resulting in mitotic arrest and subsequent apoptosis; it is widely accepted that the $G_2$/M cell cycle arrest is strongly associated with inhibition of tubulin polymerisation.[75–77] To investigate the effect of the combretastatin derivatives on cell cycle arrest, flow cytometry was used to analyse the cell cycle distribution of

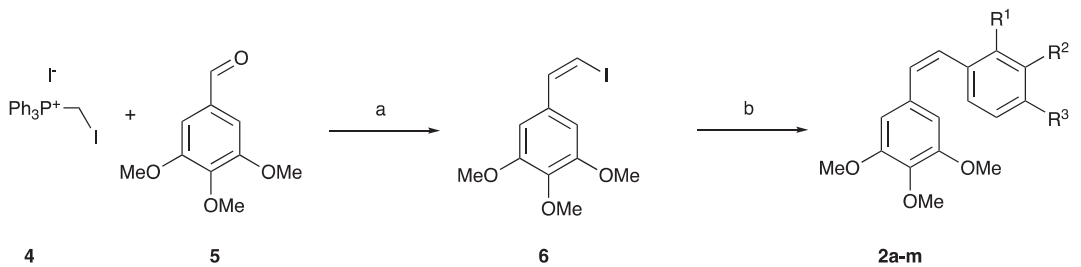


4 5 6 2a-m

**Scheme 1.** Synthesis of target compounds 2a-m Reagents and conditions: (a) NaHMDS, THF, −20 to −78 °C, 2 h; (b) arylboronic acids or pinacol esters, $Pd(PPh_3)_4$, DME, $Na_2CO_3$, 80 °C, 20 h.

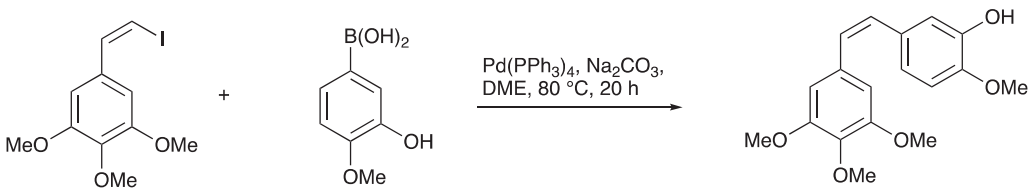


**Scheme 2.** New synthesis of Combretastatin A-4.

HepG2 cells following treatment with compounds 2a, 2b and 2e at 1 μM. Untreated cells showed a fairly even spread across the growth stages; the percentage of cells in the $G_0/G_1$ and $G_2/M$ phase were 45.6% and 44.8% respectively (table 3). After treatment with 2a, 2b and 2e, the percentage of cells in the $G_2/M$ phase drastically increased to 91.6%, 94.6% and 94.7% respectively.

After incubation for 48 h with 2a, the percentage of apoptotic cells (sub-$G_1$) increased (43.3%) and the percentage of $G_2/M$ arrested cells decreased (46.7%). The increased sub-$G_1$ population, suggested extensive DNA fragmentation indicating apoptosis as a direct result of mitotic arrest.[51] We observed a similar trend for compounds 2b and 2e after 48h; the percentage of apoptotic cells increased to 43.3% and 43.5% respectively. This cell cycle arrest in the $G_2/M$ phase and subsequently sub-$G_1$ suggests compounds 2a, 2b and 2e inhibit tubulin polymerisation causing a mitotic block that leads to apoptosis.

## 3. Conclusion

In conclusion, a series of combretastatin analogues were synthesised using a new two-step reaction by use of a Wittig olefination followed by the Suzuki cross-coupling. Fourteen compounds were synthesised using this new route including the biologically active CA-4 in a 56% overall yield. This two-step synthesis is an improved synthesis of CA-4 which allowed for a library of combretastatins with B-ring modifications to be synthesised.

**Table 2**
Rate (k) and half-life ($t_{1/2}$) of tubulin polymerisation after treatment with compounds 2d and 2g.

| Conditions | k ($min^{-1}$) | $t_{1/2}$ (min) |
|---|---|---|
| No drug control | 0.0208 | 33 |
| 2d (1 μM) | 0.0116 | 59 |
| 2g (1 μM) | 0.0123 | 56 |

**Table 3**
Effect of compounds 2a, 2b and 2e on the cell cycle in HepG2 cells.

| | 2a | | 2b | | 2e | | No drug control | |
|---|---|---|---|---|---|---|---|---|
| | 24 h | 48 h | 24 h | 48 h | 24 h | 48 h | 24 h | 48 h |
| Sub $G_1$ | 3.3 | 44.2 | 1.2 | 43.3 | 2.7 | 43.5 | 1.2 | 5.9 |
| $G_0/G_1$ | 3.5 | 5.6 | 2.8 | 21.5 | 1.6 | 11.4 | 45.6 | 56.2 |
| S | 1.6 | 3.5 | 1.3 | 4.1 | 1.0 | 4.1 | 8.4 | 12.5 |
| $G_2/M$ | 91.6 | 46.7 | 94.6 | 31.1 | 94.7 | 41.0 | 44.8 | 25.4 |

Number of cells arrested in each stage of the cell cycle are expressed as a percentage (%).

New compounds (2a-2i) exhibited antiproliferative activities in nanomolar concentrations. 4-Formyl-3′,4′,5′-trimethoxy-(Z)-stilbene (2a), 4-formyl-3-hydroxy-3′,4′,5′-trimethoxy-(Z)-stilbene (2b) and 4-

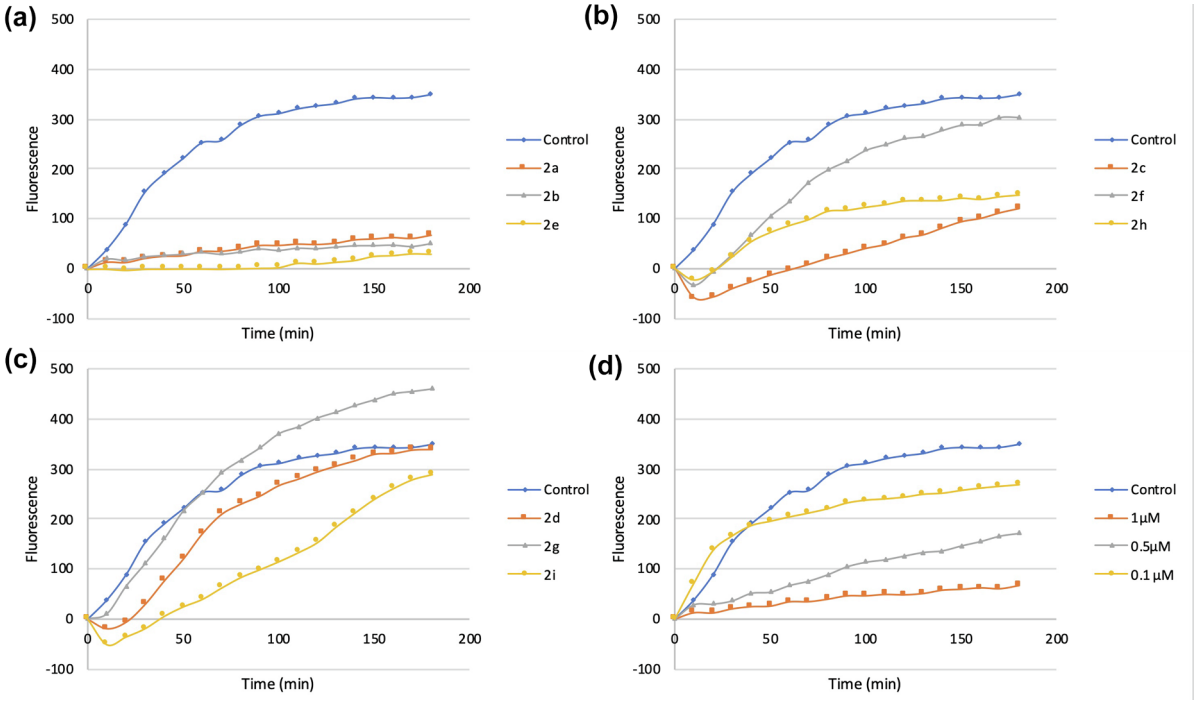


**Fig. 2.** Combretastatin derivatives (1 μM) inhibited the assembly of tubulin *in vitro*. Normal tubulin polymerisation is shown as the control. Paclitaxel (3 μM) and CA-4 (1 μM) were used as positive controls and experiments were repeated three times. Data is shown for one of these repeats. (a) Compounds 2a, 2b, 2e; (b) 2c, 2f, 2 h; (c) 2d, 2g, 2i; (d) example of dose curves for compound 2a 1 μM, 0.5 μM, 0.1 μM.

Acetyl-3′,4′,5′-trimethoxy-(Z)-stilbene (2e) were the most potent across all three cell lines. Like CA-4, compounds 2a, 2b and 2e inhibited the rate and extent of an *in vitro* assembly of purified tubulin with $IC_{50}$s of 0.39, 0.32 and 0.28 μM respectively. Additionally, compounds 2a, 2b and 2e appear to cause a mitotic block and eventual apoptosis in HepG2 cells, further confirming their ability to inhibit tubulin polymerisation.

## 4. Experimental

### 4.1. Chemistry

#### 4.1.1. General considerations

All reactants and reagents were obtained from the commercial source and used without further purification. The NMR spectra were recorded on a Bruker Avance DPX 400 MHz spectrometer in $CDCl_3$ unless stated otherwise using TMS as an internal standard. J values are given in Hz. HRMS (ESI) were recorded with Bruker–Maxis mass spectrometers. The purity of synthesized compounds was analyzed by HPLC (Shimadzu LC-6AD system), Phenomenex RP-C18 column (250 mm × 4.60 mm), particle size 5 μm, flow rate 1 ml/min, using water-acetonitrile. Purity of tested compounds was > 95%.

#### 4.1.2. Z-3,4,5-Trimethoxy-β-iodostyrene (6)[57]

A suspension of iodomethylenetriphenylphosphonium iodide (3.53 g, 6.67 mmol, 1.3 eq) in anhydrous THF (30 ml) was cooled to −20 °C and sodium bis(trimethylsilyl)amide in THF (3.33 ml of a 2 M solution, 1.3 eq) was added dropwise. The resulting mixture was stirred at −20 °C for 15 min, then cooled to −78 °C and 3,4,5-trimethoxybenzaldehyde (1 g, 1.45 mmol, 1 eq) in THF (10 ml) was added over 1 h with good stirring. The reaction was stirred for a further 2 h, quenched with saturated aq. $NH_4Cl$ (10 ml) and extracted with diethyl ether (3 × 10 ml). The combined organic layers were filtered to remove triphenylphosphine oxide, dried over $MgSO_4$ and concentrated *in vacuo*. The residue was purified by flash chromatography on silica gel (hexane/EtOAc, 4:1) to give **6** (1.2 g, 72%) as a yellow oil. $^1$H δ ppm: 7.20 (d, *J* = 8.6 Hz, 2 h), 6.91 (s, 2H), 6.48 (d, *J* = 8.6 Hz, 2 h), 3.86 (s, 6H), 3.85 (s, 3H).

#### 4.1.3. General synthesis of boronic pinacol esters[78]

Into a thick walled screw top flask containing a solution of appropriately substituted aryl halide (2.49 mmol, 1 eq) in dry 1,4-dioxane (10 ml) were added *bis*(pinacolato)diboron (0.632 g, 2.49 mmol, 1 eq) [1,1′-*Bis*(diphenylphosphino)ferrocene]palladium(II) dichloride (0.03 eq) and potassium acetate (3 eq). The flask was cooled to 0 °C under argon for 30 min. The reaction mixture was gradually warmed to room temperature, and stirred at 80 °C for 16 h. After cooling to room temperature, the solvent was evaporated to dryness under reduced pressure. The residue was dissolved in *n*-hexane, and the solution was washed with $H_2O$, brine and dried ($MgSO_4$), further purification was by recrystallization from hexane.

*4.1.3.1. 2-Hydroxy-4-(4,4,5,5-tetramethyl-1,3,2-dioxaborolan-2-yl) benzaldehyde (**7a**)*[78]. From 4-bromosalicylaldehyde (0.500 g, 2.49 mmol, 1 eq). **7a** was isolated as a white solid (0.482 g, 1.94 mmol, 78%). $^1$H δ: 1.28 (12H, s, 4 × $CH_3$), 7.35 (2 H, m), 7.48 (1 H, d, *J* = 8.16), 9.86 (1 H, s, CHO), 10.76 (1 H, s, OH).

*4.1.3.2. 2-Hydroxy-4-(4,4,5,5-tetramethyl-1,3,2-dioxaborolan-2-yl) acetophenone (**7b**)*. From 1-(4-bromo-2-hydroxyphenyl)ethanone (0.535 g, 2.49 mmol, 1 eq) **7b** was isolated as a white solid (0.451 g, 1.72 mmol, 69%). $^1$H δ: 1.28 (12H, s, 4 × $CH_3$), 2.58 (3H, s, $CH_3$), 7.22 (1H, dd, *J* = 7.87, 0.97, *para* to OH), 7.35 (1H, d, *J* = 0.97, *ortho* to OH), 7.64 (1H, d, *J* = 7.87, *meta* to OH), 11.99 (1H, s, OH); $^{13}$C δ: 24.9 (4C, $CH_3$), 26.9 (1C, $CH_3$), 84.3 (2C, C—O), 114.5 (1C, C—$COCH_3$), 119.9 (1C, Ar C), 124.6 (1C, Ar C), 124.8 (1C, C—B), 129.6 (1C, Ar C), 158.8 (1C, C—OH), 201.2 (1C, C═O)

*4.1.3.3. 2-Hydroxy-4-(4,4,5,5-tetramethyl-1,3,2-dioxaborolan-2-yl) benzonitrile (**7c**)*. From 4-bromo-2-hydroxybenzonitrile (0.493 g, 2.49 mmol, 1 eq). **7c** was isolated as a white solid (0.464 g, 1.89 mmol, 76%).$^1$H δ: 1.27 (12H, s, 4 × $CH_3$), 7.14 (1H, dd, *J* = 7.71, 1.28, *para* to OH), 7.35 (1H, d, *J* = 1.28, *ortho* to OH), 7.36 (1H, d, *J* = 7.71, *meta* to OH), 10.49 (1H, s, OH); $^{13}$C δ: 24.9 (4C, $CH_3$), 84.5 (2C, C—O), 94.6 (1C, C—CN), 105.2 (1C, C—B), 116.4 (1C, CN), 120.1 (1C Ar C), 127.9 (1C, Ar C), 132.8 (1C, Ar C), 158.2 (1C, Ar C—OH).

#### 4.1.4. Synthesis of combretastatin A-4 and analogues (**2a-i**)

*4.1.4.1. General synthesis of combretastatins*. 3,4,5-Trimethoxy-β-iodostyrene (0.22 g, 0.68 mmol, 1 eq) and *tetrakis* (triphenylphosphine) palladium(0) (0.04 g, 0.034 mmol, 5 mol %) were stirred in 1,2-dimethoxyethane (50 ml) under argon for 20 min. Aryl boronic acid (or ester) (1.02 mmol, 1.5 eq) (for 1 0.168 g, 2a 0.150 g, 2b 0.248 g, 2c 0.180 g, 2d 0.150 g, 2e 0.164 g, 2f 0.262 g, 2g 0.164 g, 2h 0.147 g, 2i 0.245g, 2j 0.167 g, 2k 0.167 g, 2l 0.212 g, 2m 0.122 g) and aqueous sodium carbonate (1 ml of a 2 M solution, 3 eq) were added and the mixture heated at reflux for 20 h. The reaction mixture was allowed to cool to room temperature, passed through a plug of celite and the DME was removed *in vacuo*. DCM (20 ml) was added and washed with saturated brine, water, dried ($MgSO_4$), and concentrated *in vacuo*. The residue was purified by flash column chromatography on silica gel (petroleum ether/EtOAc 10:1) and recrystallised from methanol.

*4.1.4.2. Combretastatin A-4 (**1**)*[52]. From 3-methoxy-4-hydroxyphenyl boronic acid (0.168 g, 1 mmol, 1.5 eq). Following purification **1** was isolated as a white solid (0.168 g, 78%); Mp 117–118 (lit. mp[41] 116–118). $^1$H δ: 3.70 (6H, s, 2 × OMe), 3.85, 3.87 (6H, 2 s, 2 × OMe), 5.55 (1H, s, OH), 6.43, 6.49 (2H, 2 d, *J* = 12.2 Hz, olefinic Hs), 6.67 (2H, s, ArH ortho to OMe), 6.85 (1H, d, *J* = 8 Hz, ArH meta to OH), 6.80 (1H, dd, *J* = 8, 2 Hz, ArH para to OH), 6.93 (1H, d, *J* = 2 Hz, ArH ortho to OH).

*4.1.4.3. 4-Formyl-3′,4′,5′-trimethoxy-(Z)-stilbene (**2a**)*[79]. From 4-formylphenyl boronic acid (0.15 g, 1 mmol, 1.5 eq). Following purification **2a** was isolated as yellow crystals (0.171 g, 84%); Mp 98–100 °C; $^1$H δ: 3.57 (3H, s, 4′-OMe), 3.70 (6H, s, 3′,5′-OMe), 6.37 (2H, s, 2′,6′-CH), 6.51 (1H, d, *J* = 12.3, olefinic CH), 6.58 (1H, d, *J* = 12.3, olefinic CH), 7.37 (2H, d, *J* = 8.2, 2, 6-CH), 7.69 (2H, d, *J* = 8.2, 3, 5-CH), 9.08 (1H, s, CHO). $^{13}$C (100 MHz) *δ* 55.9, (2 × $OCH_3$), 60.9 ($OCH_3$), 106.1 (2,6-C), 125.5 (2′,6′-C), 128.6, 129.6 (2 × olefinic CH), 130.1 (3′,5′-C), 131.8 (1-C), 135.0 (4′-C), 137.7 (1′-C), 140.0 (4-C), 153.0 (3,5-C), 191.5 (CHO). HRMS calcd for $C_{18}H_{19}O_4$ [M + $H^+$]: 299.1278; found: 299.1278.

*4.1.4.4. 4-Formyl-3-hydroxy-3′,4′,5′-trimethoxy-(Z)-stilbene (**2b**)*. From 2-hydroxy-4-(4,4,5,5-tetramethyl-1,3,2-dioxaborolan-2-yl) benzaldehyde (0.248 g, 1.00 mmol). Following purification **2b** was isolated as a pale yellow solid (0.113 g, 54%); Mp 89 °C. $^1$H δ: 3.71 (3H, s, $OCH_3$), 3.87 (6H, s, 2 × $OCH_3$), 6.50 (2H, s, Ar H), 6.51 (1H, d, *J* = 12.3, CH), 6.53 (1H, d, *J* = 12.3, CH), 6.68 (1H, dd, *J* = 7.7, 1.8, *para* to OH), 6.69 (1H, d, *J* = 1.8, *ortho* to OH), 7.43 (1H, d, *J* = 7.7, *meta* to OH), 9.83 (1H, s, CHO), 11.06 (1H, s, OH).$^{13}$C (100 MHz) *δ* 56.2 (2C, 2 × $OCH_3$), 61.0 (1C, $OCH_3$), 104.2 (1C, o—OH), 106.2 (2C, o—C—$OCH_3$), 114.8 (1C, C—CHO), 126.6 (1C, o—CHO), 128.3 (1C, p—OH) 131.6 (1C, ArC), 132.0 (2C, CH), 138.9 (1C, C—O $CH_3$), 153.0 (2C, C—O $CH_3$), 153.5 (1C, C—OH), 195.7 (1C, C═O). HRMS calcd for $C_{18}H_{19}O_5$ 315.1230, found 315.1227.

*4.1.4.5. 2-Formyl-3′,4,4′,5′-tetramethoxy-(Z)-stilbene (**2c**)*. From 2-formylphenyl boronic acid (0.18 g, 1 mmol, 1.5 eq). Following purification **2c** was isolated as a pale yellow solid (0.176 g, 79%); Mp 88–91 °C; $^1$H δ: 3.60 (3H, s, 4′-OMe), 3.82 (6H, s, 3′,5′-OMe), 3.88

(3H, s, 4-OMe), 6.31 (2H, s, 2′,6′-CH), 6.72 (1H, d, $J$ = 12.2, olefinic CH), 6.88 (1H, d, $J$ = 12.2, olefinic CH), 7.13 (1H, dd, $J$ = 2.9, 8.6, 5-CH), 7.28 (1H, d, $J$ = 8.6, 6-CH), 7.43 (1H, d, $J$ = 2.9, 3-CH), 10.25 (1H, s, CHO). $^{13}$C (100 MHz) $\delta$ 55.6, 55.8 (4, 4′-OMe), 60.9 (3′,5′-OMe), 106.4 (2,6-C), 110.9 (3′-C), 114.6 (5′-C), 121.7 (6′-C), 125.2, 131.3 (2 × olefinic Cs), 131.9 (1-C), 133.3 (2′-C), 134.2 (2′-C), 134.4 (1′-C), 139.4 (4-C), 152.9 (3,5-Cs), 159.1 (4′-C), 191.7 (CHO). HRMS calcd for $C_{19}H_{21}O_5$ [M + $H^+$]: 329.1384; found: 329.1385.

*4.1.4.6. 2-Formyl-3′,4′,5′-trimethoxy-(Z)-stilbene* ***(2d)***. From 2-formylphenyl boronic acid (0.15 g, 1 mmol, 1.5 eq). Following purification 2d was isolated as a yellow solid (0.162 g, 80%); Mp 91–93 °C; $^1$H δ: 3.48 (3H, s, 4′-OMe), 3.71 (6H, s, 3′,5′-OMe), 6.15 (2H, s, 1′,6′-CHs), 6.66 (1H, d, $J$ = 12.5, olefinic CH), 6.86 (1H, d, $J$ = 12.5, olefinic CH), 7.27 (1H, d, $J$ = 7.5, 4-CH), 7,34 (1H t, $J$ = 7.5, 6-CH), 7.47 (1H, m, 5-CH), 7.85 (1H, d, $J$ = 7.5, 3-CH). $^{13}$C (100 MHz) $\delta$ 56.2 (2 × $OCH_3$), 60.9 ($OCH_3$), 104.1 (2,6-Cs), 125.8 (6′-C), 127.2, 127.7 (2 × olefinic CH), 128.9 (3′-C), 130.6 (4′-C), 131.1 (5′-C), 133.3 (1-C), 134.0 (1′-C), 137.6 (2′-C), 141.5 (4-C), 153.5 (3,5-Cs), 192.0 (CHO). HRMS calcd for $C_{18}H_{19}O_4$ [M + $H^+$]: 299.1278; found: 299.1278.

*4.1.4.7. 4-Acetyl-3′,4′,5′-trimethoxy-(Z)-stilbene* ***(2e)***. From 4-acetylphenylboronic acid (0.164 g, 1 mmol, 1.5 eq). Following purification 2e was isolated as a white solid (0.157 g, 74%); Mp 79–81 °C; $^1$H δ: 2.51 (3H, s, OCMe), 3.59 (6H, s, 3′,5′-OMes), 3.77 (3H, s, 4′-OMe), 6.38 (2H, s, 2′,6′-CH), 6.51 (1H, d, $J$ = 12.3, olefinic CH), 6.57 (1H, d, $J$ = 12.3, olefinic CH), 7.31 (2H, d, $J$ = 8.1, 2, 6-CH), 7.78 (2H, d, $J$ = 8.2, 3,5-CH); $^{13}$C (100 MHz) $\delta$ 26.4 (4′-OC*Me*), 55.9 (3′,5′-OMes), 61.0 (4-OMe), 106.1 (2,6-C), 128.3 (olefinic C), 128.4 (2′,6′-C), 128.8 (olefinic C), 129.1 (3′,5′-C), 132.3 (1-C), 137.4 (4′-C), 139.5 (4-C), 143.5 (1′-C), 153.0 (3,5-C), 193.5 (CHO). HRMS calcd for $C_{19}H_{21}O_4$ [M + $H^+$]: 313.1431; found: 313.1434.

*4.1.4.8. 4-Acetyl-3-hydroxy-3′,4′,5′-trimethoxy-(Z)-stilbene* ***(2f)***. From and 2-hydroxy-4-(4,4,5,5-tetramethyl-1,3,2-dioxaborolan-2-yl)acetophenone (0.262 g, 1.00 mmol). Following purification **2f** was isolated as a pale yellow solid (0.122 g, 56%). Mp 73 °C. $^1$H δ: 2.62 (3H, $CH_3$), 3.72 (6H, s, 2 × $OCH_3$), 3.87 (3H, s, $OCH_3$) , 6.51 (2H, s, Ar H), 6.52 (1H, d, $J$ = 12.5, CH), 6.66 (1H, d, $J$ = 12.5, CH), 6.83 (1H, dd, $J$ = 8.2, 1.6, *para* to OH), 6.97 (1H, d, $J$ = 1.6, *ortho* to OH), 7.60 (1H, d, $J$ = 8.2, *meta* to OH), 12.27 (1H, s, OH). $^{13}$C (100 MHz) $\delta$ 26.6 (1C, $CH_3$), 56.0 (2C, 2 × $OCH_3$), 61.0 (1C, $OCH_3$), 106.2 (2C, o—C—$OCH_3$), 118.3 (C—$COCH_3$), 128.5 (1C, o—$COCH_3$), 130.3 (1C, p—OH), 131.8 (1C, ArC), 132.9 (1C, Ar C), 146.0 (1C, C—$OCH_3$), 153.0 (2C, C—O $CH_3$), 162.4 (1C, C—OH), 203.8 (1C, C═O). HRMS calcd for $C_{19}H_{21}O_5$ [M + H]: 329.1384; found: 329.1385.

*4.1.4.9. 2-Acetyl-3′,4′,5′-trimethoxy-(Z)-stilbene* ***(2g)***. From 5-[(Z)-2-bromovinyl]-1,2,3-trimethoxybenzene (0.164 g, 1 mmol, 1.5 eq).) and 2-acetylphenylboronic acid (0.169 g, 1.03 mmol). Following purification **2g** was isolated as a yellow solid (0.182 g, 0.58 mmol, 85%).$^1$H δ: 2.56 (3H, s, $CH_3$), 3.60 (6H, s, 2 × $OCH_3$), 3.82 (3H, s, $OCH_3$), 6.28 (2H, s, Ar H), 6.56 (1H, d, $J$ = 12.3, CH), 6.92 (1H, d, $J$ = 12.3, CH), 7.33 (2H, d, $J$ = 7.4, Ar H) 7.36 (t, $J$ = 1.58, 8.99, 1H, Ar H), 7.79 (d, J = 7,4 , 1H, Ar H); $^{13}$C (100 MHz) $\delta$ 29.5 ($CH_3$), 55.7 (2C, $OCH_3$), 60.9 ($OCH_3$), 106.4 (olefinic C), 126.7 (Ar C), 127.7 (Ar C), 129.1 (olefinic C), 129.9 (olefinic C), 130.0 (Ar C), 131.2 (Ar C), 131.6 (Ar C), 132.0 (Ar C), 137.2 (Ar C), 138.0 (Ar C). 152.7 (olefinic C), 200.7 (carbonyl C). HRMS calcd for $C_{19}H_{21}O_4$ [M + H]: 313.1431, found: 313.1434.

*4.1.4.10. 4-Cyano-3′,4′,5′-trimethoxy-(Z)-stilbene* ***(2h)***. From 4-cyanophenylboronic acid (0.147 g, 1 mmol, 1.5 eq). Following purification 2h was isolated as a white solid (0.156 g, 78%); Mp 89–91 °C. $^1$H δ: 3.60 (s, 6H), 3.78 (s, 3H), 6.33 (s, 2H), 6.47 (d, $J$ = 12.2, 1H), 6.60 (d, $J$ = 12.2, 1H), 7.31 (d, $J$ = 8.4, 2H), 7,47 (d, $J$ = 8.4, 2H). $^{13}$C (100 MHz) 55.9 (3′,5′ OMe), 61.0 (4′-OMe), 106. 0 (2′, 6′-C), 110.5 (1-C), 118.9 (1′-C), 128.0, 129.7 (2 × olefinic C), 131.5 (CN), 132.4 (2, 6-C), 133.10 (3,5-C), 137.8 (4′-C), 142.3 (aromatic 4-C), 153.1 (3′, 5′-C). HRMS calcd for $C_{18}H_{18}NO_3$ [M + $H^+$]: 296.1287; found: 296.1281.

*4.1.4.11. 4-Cyano-3-hydroxy-3′,4′,5′-trimethoxy-(Z)-stilbene* ***(2i)***. From 2-hydroxy-4-(4,4,5,5-tetramethyl-1,3,2-dioxaborolan-2-yl)benzonitrile (0.245 g, 2.00 mmol. Following purification, **2i** was isolated as a dark yellow solid (0.100 g, 48%). Mp 95 °C. $^1$H δ: 3.70 (6H, s, 2 × $OCH_3$), 3.85 (3H, s, $OCH_3$) , 6.45 (2H, s, Ar H), 6.48 (1H, d, $J$ = 12.2, CH), 6.63 (1H, d, $J$ = 12.2, CH), 6.88 (1H, dd, $J$ = 9.0, 1.2, *para* to OH), 6.98 (1H, d, $J$ = 1.2, *ortho* to OH), 7.39 (1H, d, $J$ = 9.0, *meta* to OH). $^{13}$C (100 MHz) $\delta$ 55.9 (2C, 2 × $OCH_3$), 61.2 (1C, $OCH_3$),99.8 (1C, C—CN), 106.0 (2C, o—C—$OCH_3$), 121.4 (CN), 128.1 (1C, o—$COCH_3$), 1331.5 (1C, p—OH), 132.8 (1C, ArC), 132.9 (1C, Ar C), 143.9 (1C, C—$OCH_3$), 153.1 (2C, C—O $CH_3$), 159.4 (1C, C—OH). HRMS calcd for $C_{18}H_{16}NO_4$ 3[M-H]:10.33, found 310.00.

*4.1.4.12. 4-Nitro-3′,4′,5′-trimethoxy-(Z)-stilbene* ***(2j)***[80]. From 4-nitrophenyl boronic acid (0.167 g, 1 mmol, 1.5 eq). Following purification 2j was isolated as a yellow solid (0.167 g, 78%); Mp 142–143 °C. (Lit. Mp 210–212 °C). $^1$H δ: 3.70 (6H, s, 3′,5′-OMe), 3.88 (3H, s, 4-OMe), 6.51 (1H, d, $J$ = 12.0, olefinic H), 6.25 (1H, d, $J$ = 12.0, olefinic H), 6.45 (2H, s, 2′, 6′-CHs), 7.48 (2H, d, $J$ = 8.1, 2,6-CHs), 8.15 (2H, d, $J$ = 8.1, 3,5-CHs).

*4.1.4.13. 2-Nitro-3′,4′,5′-trimethoxy-(Z)-stilbene* ***(2k)***[81]. From 2-nitrophenyl boronic acid (0.167 g, 1 mmol, 1.5 eq). Following purification 2k was isolated as a yellow solid (0.158 g, 74%); Mp 126–129 °C. $^1$H δ: 3.60 (6H, s, 3′, 5′-OMe), 3.82 (3H, s, 4′-OMe), 6.38 (2H, s, 2′,6′-CHs), 6.69 (d, $J$ = 12.1, olefinic H), 6.90 (d, $J$ = 12.1, olefinic H), 7.38 (1H, d, $J$ = 8.2, 3-CH), 7.42 (1H, m, 4-CH), 7.48 (1H, m, 5-CH), 8.10 (1.0, d, $J$ = 8.2, 6-CH).

*4.1.4.14. 3,3′,4,4′,5,5′-Hexamethoxy-(Z)-stilbene* ***(2l)***[82]. From 3,4,5-trimethoxyphenyl boronic acid (0.212 g, 1 mmol, 1.5 eq). Following purification 2l was isolated as a white solid (0.181 g, 0.5 mmol, 74%); Mp 173–175 °C. (Lit. Mp 173 °C). $^1$H δ: 3.72 (12H, s, 3,3′,5,5′-OMe), 3.85 (6H, s, 4,4′-OMe), 6.52 (2 H, s, 2 × olefinic Hs) 2 H), 6.53 (4 H, s, 2,2′,6,6′-CHs)).

*4.1.4.15. 3,4,5-Trimethoxy-(Z)-stilbene* ***(2m)***[83]. From phenylboronic acid (0.122 g, 1 mmol, 1.5 eq). Following purification **2m** was isolated as a yellow solid (0.149 g, 81%); Mp 105–107 °C. (Lit. mp 106–8 °C. $^1$H δ: 3.69 (3H, s, 4-OMe), 3.85 (6H, s, 3,5-OMes), 6.47 (2H, s, 2,6-Hs), 6.54 (1H, d, $J$ = 12.2, olefinic H), 6.62 (1H, d, $J$ = 12.2, olefinic H), 7.22–7.32(5H, m, 2′,3′,4′,5,6′-Hs).

### 4.2. Biology

#### 4.2.1. Cell culture

HepG2, HeLa and HCT-116 cells were cultured in Dulbecco's Modified Eagle's Medium (DMEM) supplemented with FCS (10%), penicillin (100 units/ml), streptomycin (100 μg/ml) and L-glutamine (2 mM). Cell lines were cultured at 37 °C in a humidified incubator with 5% carbon dioxide.

#### 4.2.2. Cell-based screening assay

Synthesized combretastatin analogues, (**2a**-**2i**) and CA-4 used in the study were dissolved in 100% cell culture grade DMSO. The compounds were serially diluted in DMEM to maintain the final concentration of DMSO as < 0.1% for testing on cancer cell lines. A concentration of 50 μM of synthesized combretastatin analogues (**2a**-**2i**) and CA-4 were initially used for screening the potency of compounds in cell lines.

#### 4.2.3. Half-Maximal Inhibition of Tumour Cell Growth by Combretastatin Analogues

HepG2, HeLa and HCT-116 cells ($1 \times 10^5$ cells/mL) were seeded in 96-well plates and incubated for 24 h for attachment. The cells were then incubated with different concentrations of synthesized combretastatin analogues and incubated for 24 h. Following incubation, MTT solution (50 µl; 3 mg/ml in PBS) was added to each well and incubated for a further 3 h. The half-maximal inhibitory concentration ($IC_{50}$) for the respective compounds were determined using a known method. In short, formazan crystals were dissolved in DMSO (100 µl) and optical densities of the wells were read on a spectrophotometer platereader (Multiskan Ascent, Thermo Labsystems) at 540 nm with 690 nm as a background reading. The no drug control sample was normalised to 100% cell growth (no inhibition of cell growth). CA-4 was used as a control for comparing the potencies of the synthesized combretastatin analogues. Data was analysed using GraphPad. 6 sets of experiments were performed.

#### 4.2.4. Assembly Kinetics of Tubulin in vitro

A fluorescence-based tubulin polymerisation assay was performed according to the manufacturer's protocol (cat # BK011P, Cytoskeleton, Inc.). Tubulin (10 mg $ml^{-1}$) was resuspended in a premixed buffer containing PIPES, EGTA, $MgCl_2$ and fluorescent reporter (243 µl), glycerol buffer (112 µl) and GTP (100 mM, 4.4 µl). The tubulin reaction mix (50 µl) was added to 1 µM of test compounds and subsequently the assembly kinetics of tubulin was monitored using excitation wavelength 355 nm at 37 °C using Spectramax M2. CA4 and paclitaxel were tested as controls and three independent experiments were performed for each compound.

#### 4.2.5. Cell cycle analysis by flow cytometry

HepG2 cells were incubated in the absence and presence of compounds 2a, 2b, 2e and CA-4 for 24 h or 48 h. Subsequently, the cells were fixed with 70% ethanol. The fixed cells were then incubated with RNase (50 µl; 100 µg/ml in PBS) and propidium iodide (300 µl; 50 µg/ml in PBS) for 1 h. Flow cytometry analysis was performed using BD FACSVerse flow cytometer.

## Declaration of Competing Interest

The authors declare that they have no known competing financial interests or personal relationships that could have appeared to influence the work reported in this paper.

## Acknowledgements

We thank Roger Bisby for his help with the tubulin assay and Kirit Amin (Salford Analytical Services) for technical assistance. We thank the EPSRC, UK, grant 1817912 National Mass Spectrometry Service at Swansea University for mass spectrometry services. Kidscan - Children's Cancer Research, UK, grant KGR14.

## References

1. Jordan A, Hadfield JA, Lawrence NJ, McGown AT. Tubulin as a target for anticancer drugs: agents which interact with the mitotic spindle. *Med Res Rev.* 1998;18:259–296.
2. Hadfield JA, Ducki S, Hirst N, McGown AT. Tubulin and microtubules as targets for anticancer drugs. *Prog Cell Cycle Res.* 2003;5:309–325.
3. Jordan MA, Wilson L. Microtubules as a target for anticancer drugs. *Nat Rev Cancer.* 2004;4:253–265. https://doi.org/10.1038/nrc1317.
4. Mukhtar E, Adhami VM, Mukhtar H. Targeting microtubules by natural agents for cancer therapy. *Mol Cancer Ther.* 2014;13:275–284. https://doi.org/10.1158/1535-7163.MCT-13-0791.
5. Lin CM, Ho HH, Pettit GR, Hamel E. Antimitotic natural products combretastatin A-4 and combretastatin A-2: studies on the mechanism of their inhibition of the binding of colchicine to tubulin. *Biochemistry.* 1989;28:6984–6991. https://doi.org/10.1021/bi00443a031.
6. Uppalapati M, Huang Y, Aravamuthan V, Jackson TN, Hancock WO. Integrative biology "' Artificial Mitotic Spindle "' generated by dielectrophoresis and protein micropatterning supports bidirectional transport of Kinesin-coated beadsw. *Integrative Biol.* 2011:57–64. https://doi.org/10.1039/c0ib00065e.
7. Weaver BA. How taxol/paclitaxel kills cancer cells. *Mol Biol Cell.* 2014;25:2677–2681. https://doi.org/10.1091/mbc.E14-04-0916.
8. Nam N-H. Combretastatin A-4 analogues as antimitotic antitumor agents. *Curr Med Chem.* 2003;10:1697–1722.
9. Liu YQ, Tian J, Qian K, et al. Recent progress on C-4-modified podophyllotoxin analogs as potent antitumor agents. *Med Res Rev.* 2015;35:1–62. https://doi.org/10.1002/med.21319.
10. Sessa C, Lorusso P, Tolcher A, et al. Phase I safety, pharmacokinetic and pharmacodynamic evaluation of the vascular disrupting agent ombrabulin (AVE8062) in patients with advanced solid tumors. *Clin Cancer Res.* 2013;19:4832–4842. https://doi.org/10.1158/1078-0432.CCR-13-0427.
11. Ho YJ, Wang TC, Fan CH, Yeh CK. Current progress in antivascular tumor therapy. *Drug Discovery Today.* 2017;22:1503–1515. https://doi.org/10.1016/j.drudis.2017.06.001.
12. Nishio M, Satouchi M, Horiike A, et al. Phase 1 study of ombrabulin in combination with docetaxel and cisplatin in japanese patients with advanced solid tumors. *JJCO Jpn J Clin Oncol Jpn J Clin Oncol.* 2018;48:322–328. https://doi.org/10.1093/jjco/hyy026.
13. Gill JH, Rockley KL, De Santis C, Mohamed AK. Vascular disrupting agents in cancer treatment: cardiovascular toxicity and implications for co-administration with other cancer chemotherapeutics. *Pharmacol Ther.* 2019;202:18–31. https://doi.org/10.1016/j.pharmthera.2019.06.001.
14. Qin H, Yu H, Sheng J, et al. PI3Kgamma inhibitor attenuates immunosuppressive effect of poly(L-glutamic acid)-combretastatin A4 conjugate in metastatic breast cancer. *Adv Sci.* 2019;6:1900327. https://doi.org/10.1002/advs.201900327.
15. Hong S, Zheng DW, Zhang C, Huang QX, Cheng SX, Zhang XZ. Vascular disrupting agent induced aggregation of gold nanoparticles for photothermally enhanced tumor vascular disruption. *Sci Adv.* 2020;6:1–12. https://doi.org/10.1126/sciadv.abb0020.
16. Pettit GR, Cragg GM, Herald DL, Schmidt JM, Lohavanijaya P. Isolation and structure of combretastatin. *Can J Chem.* 1982;60:1374–1376. https://doi.org/10.1139/v82-202.
17. Nasir S, Bukhari A, Kumar GB, Revankar HM, Qin H-L. Development of combretastatins as potent tubulin polymerization inhibitors. *Bioorg Chem.* 2017;72:130–147. https://doi.org/10.1016/j.bioorg.2017.04.007.
18. Ley CD, Horsman MR, Kristjansen PEG. Early effects of combretastatin-A4 disodium phosphate on tumor perfusion and interstitial fluid pressure. *Neoplasia.* 2007;9:108–112. https://doi.org/10.1593/NEO.06733.
19. Ahmed B, Van Eijk LI, Bouma-ter Steege JC, et al. Vascular targeting effect of combretastatin A-4 phosphate dominates the inherent angiogenesis inhibitory activity. *Int J Cancer.* 2003;105:20–25. https://doi.org/10.1002/ijc.11010.
20. Böhle AS, Leuschner I, Kalthoff H, Henne-Bruns D. Combretastatin A-4 prodrug: a potent inhibitor of malignant hemangioendothelioma cell proliferation. *Int J Cancer.* 2000;87:838–843. https://doi.org/10.1002/1097-0215(20000915)87:6<838::AID-IJC13>3.0.CO;2-7.
21. Jain RK, Carmeliet PF. Vessels of death or life. *Sci Am.* 2001:38–45.
22. Patterson DM, Rustin GJS. Vascular damaging agents. *Clin Oncol.* 2007;19:443–456. https://doi.org/10.1016/j.clon.2007.03.014.
23. Chaplin DJ, Horsman MR, Siemann DW. Current development status of small-molecule vascular disrupting agents. *Curr Opin Invest Drugs.* 2006;7:522–528.
24. Hadimani MB, Hua J, Jonklaas MD, et al. Synthesis, in vitro, and in vivo evaluation of phosphate ester derivatives of combretastatin A-4. *Bioorg Med Chem Lett.* 2003;13:1505–1508. https://doi.org/10.1016/S0960-894X(03)00206-3.
25. Nathan P, Zweifel M, Padhani AR, et al. Phase I trial of combretastatin A4 phosphate (CA4P) in combination with bevacizumab in patients with advanced cancer. *Clin Cancer Res.* 2012;18:3428–3439. https://doi.org/10.1158/1078-0432.CCR-11-3376.
26. Griggs J, Metcalfe JC, Hesketh R. Targeting tumour vasculature: the development of combretastatin A4. *Lancet.* 2001;2.
27. Griggs J, Hesketh R, Smith GA, et al. Combretastatin-A4 disrupts neovascular development in non-neoplastic tissue. *Br J Cancer.* 2001;84:832–835.
28. Grosios K, Holwell SE, McGown AT, Pettit GR, Bibby MC. In vivo and in vitro evaluation of combretastatin A-4 and its sodium phosphate prodrug. *Br J Cancer.* 1999;81:1318–1327.
29. Cancer Research UK. A trial looking at immunotherapy and combretastatin for advanced bowel and pancreatic cancer (A5B7-CA4P; PH1/092).
30. Chaplin DJ, Hill SA. The development of Combretastatin A4 phosphate as a vascular targeting agent. *Int J Radiat Oncol Biol Phys.* 2002;54(5):1491–1496. https://doi.org/10.1016/S0360-3016(02)03924-X.
31. Grosios K, Loadman PM, Swaine DJ, Pettit GR, Bibby MC. Combination chemotherapy with combretastatin A-4 phosphate and 5-fluorouracil in an experimental murine colon adenocarcinoma. *Anticancer Res.* 2000;20:229–233.
32. Siemann DW, Mercer E, Lepler S, Rojiani AM. Vascular targeting agents enhance chemotherapeutic agent activities in solid tumor therapy. *Int J Cancer.* 2002;99:1–6.
33. Morinaga Y, Suga Y, Ehara S, Harada K, Nihei Y, Suzuki M. Combination effect of AC-7700, a novel combretastatin A-4 derivative, and cisplatin against murine and human tumors in vivo. *Cancer Sci.* 2003;94:200–204. https://doi.org/10.1111/j.1349-7006.2003.tb01419.x.
34. Yeung S-CJ, She M, Yang H, Pan J, Sun L, Chaplin D. Combination chemotherapy including combretastatin A4 phosphate and paclitaxel is effective against anaplastic thyroid cancer in a nude mouse xenograft model. *J Clin Endocrinol Metab.* 2007;92:2902–2909. https://doi.org/10.1210/jc.2007-0027.
35. Horsman MR, Murata R, Breidahl T, et al. Combretastatins novel vascular targeting drugs for improving anti-cancer therapy. combretastatins and conventional therapy. *Adv Exp Med Biol.* 2000;476:311–323.
36. Horsman MR, Murata R. Combination of vascular targeting agents with thermal or

radiation therapy. *Int J Radiat Oncol.* 2002;54:1518–1523. https://doi.org/10.1016/S0360-3016(02)03926-3.
37. Zweifel M, Jayson GC, Reed NS, et al. Carboplatin, and paclitaxel in patients with platinum-resistant ovarian. *Cancer.* 2011. https://doi.org/10.1093/annonc/mdq708.
38. Grisham R, Ky B, Tewari KS, Chaplin DJ, Walker J. Clinical trial experience with CA4P anticancer therapy: focus on efficacy, cardiovascular adverse events and hypertension management. *Gynecol Oncol Res Pract.* 2018;5. https://doi.org/10.1186/s40661-017-0058-5.
39. Uckun FM, Cogle CR, Lin TL, et al. A phase 1B clinical study of combretastatin A1 diphosphate (OXI4503) and cytarabine (ARA-C) in combination (OXA) for patients with relapsed or refractory acute myeloid leukemia. *Cancers (Basel).* 2020;12:11. https://doi.org/10.3390/cancers12010074.
40. Cogle CR, Collins B, Turner D, et al. Safety, feasibility and preliminary efficacy of single agent Combretastatin A1 diphosphate (OXi4503) in patients with relapsed or refractory acute myeloid leukemia or myelodysplastic syndromes. *Br J Haematol.* 2020;189:e211–e213. https://doi.org/10.1111/bjh.16629.
41. Scherer KM, Bisby RH, Botchway SW, Hadfield JA, Parker AW. Anticancer phototherapy using activation of E-combretastatins by two-photon–induced isomerization. *J Biomed Opt.* 2014;20:051004. https://doi.org/10.1117/1.jbo.20.5.051004.
42. Scherer MK, Bisby HR, Botchway WS, Parker WA. New approaches to photodynamic therapy from Types I, II and III to Type IV using one or more photons. *Anticancer Agents Med Chem.* 2017;17:171–189. https://doi.org/10.2174/1871520616666160513131723.
43. Romagnoli R, Baraldi PG, Prencipe F, et al. Design and synthesis of potent in vitro and in vivo anticancer agents based on 1-(3′,4′,5′-trimethoxyphenyl)-2-aryl-1H-imidazole. *Sci Rep.* 2016;6:26602. https://doi.org/10.1038/srep26602.
44. Brown AW, Fisher M, Tozer GM, Kanthou C, Harrity JPA. Sydnone cycloaddition route to pyrazole-based analogs of combretastatin A4. *J Med Chem.* 2016;59:9473–9488. https://doi.org/10.1021/acs.jmedchem.6b01128.
45. Madadi NR, Penthala NR, Howk K, et al. Synthesis and biological evaluation of novel 4,5-disubstituted 2H–1,2,3-triazoles as cis-constrained analogues of combretastatin A-4. *Eur J Med Chem.* 2015;103:123–132. https://doi.org/10.1016/j.ejmech.2015.08.041.
46. Ashraf M, Shaik TB, Malik MS, et al. Design and synthesis of cis-restricted benzimidazole and benzothiazole mimics of combretastatin A-4 as antimitotic agents with apoptosis inducing ability. *Bioorg Med Chem Lett.* 2016;26:4527–4535. https://doi.org/10.1016/J.BMCL.2016.06.044.
47. Kamal A, Shaik AB, Polepalli S, et al. Synthesis of arylpyrazole linked benzimidazole conjugates as potential microtubule disruptors. *Bioorg Med Chem.* 2015;23:1082–1095. https://doi.org/10.1016/j.bmc.2015.01.004.
48. Mahal K, Biersack B, Schruefer S, et al. Combretastatin A-4 derived 5-(1-methyl-4-phenyl-imidazol-5-Yl)indoles with superior cytotoxic and anti-vascular effects on chemoresistant cancer cells and tumors. *Eur J Med Chem.* 2016;118:9–20. https://doi.org/10.1016/j.ejmech.2016.04.045.
49. Simoni D, Romagnoli R, Baruchello R, et al. Novel A-ring and B-ring modified combretastatin A-4 (CA-4) analogues endowed with interesting cytotoxic activity. *J Med Chem.* 2008;51:6211–6215. https://doi.org/10.1021/jm8005004.
50. Kamal A, Shaik B, Nayak VL, et al. Synthesis and biological evaluation of 1,2,3-triazole linked aminocombretastatin conjugates as mitochondrial mediated apoptosis inducers. *Bioorg Med Chem.* 2014;22:5155–5167. https://doi.org/10.1016/j.bmc.2014.08.008.
51. Gerova MS, Stateva SR, Radonova EM, et al. Combretastatin A-4 analogues with benzoxazolone scaffold: synthesis, structure and biological activity. *Eur J Med Chem.* 2016;120:121–133. https://doi.org/10.1016/j.ejmech.2016.05.012.
52. Petit GR, Singh SB, Boyd MR, et al. Antineoplastic agents. 291, Isolation and synthesis of combretastatins A-4, A-5, and A-6. *J. Med. Chem.* 1995;38:1666–1672.
53. Lawrence NJ, Ghani FA, Hepworth LA, Hadfield JA, McGown AT, Pritchard RG. The synthesis of (E) and (Z)-combretastatins A-4 and a phenanthrene from combretum caffrum. *Synthesis (Stuttg).* 1999;9:1656–1660.
54. Fürstner A, Nikolakis K. Ethynylation of aryl halides by a modified suzuki reaction. Application to the syntheses of combretastatin A-4, A-5, and lunularic acid. *Liebigs Ann.* 1996;12:2107–2113. https://doi.org/10.1002/jlac.199619961224.
55. Gaukroger K, Hadfield JA, Hepworth LA, Lawrence NJ, McGown AT. Novel syntheses of cis and trans isomers of combretastatin A-4. *J Org Chem.* 2001;66:8135–8138.
56. Camacho-Dávila AA. Kumada-Corriu cross coupling route to the anti-cancer agent combretastatin A-4. *Synth Commun.* 2008;38:3823–3833. https://doi.org/10.1080/00397910802238692.
57. Malysheva YB, Combes S, Fedorov AY, Knochel P, Gavryushin AE. New method of synthesis and biological evaluation of some Combretastatin A-4 analogues. *Synlett.* 2012;23:1205–1208. https://doi.org/10.1055/s-0031-1290899.
58. Robinson JE, Taylor RJK. A Ramberg-Bäcklund route to the stilbenoid anti-cancer agents Combretastatin A-4 and DMU-212. *Chem Commun (Camb).* 2007;16:1617–1619. https://doi.org/10.1039/b702411h.
59. Ishiyama T, Murata M, Miyaura N. Palladium(0)-catalyzed cross-coupling reaction of alkoxydiboron with haloarenes: a direct procedure for arylboronic esters. *J Org Chem.* 1995;60:7508–7510. https://doi.org/10.1021/jo00128a024.
60. Stork G, Zhao K. A Stereoselective synthesis of (Z)-1-iodo-1-alkenes. *Tetrahedron Lett.* 1989;30:2173–2174. https://doi.org/10.1016/S0040-4039(00)99640-0.
61. Lennox AJJ, Lloyd-Jones GC. Selection of Boron Reagents for Suzuki-Miyaura Coupling. *Chem Soc Rev.* 2014;43:412–443. https://doi.org/10.1039/C3CS60197H.
62. Qi Z-Y, Hao S-Y, Tian H-Z, Bian H-L, Hui L, Chen S-W. Synthesis and biological evaluation of 1-(benzofuran-3-Yl)-4-(3,4,5-trimethoxyphenyl)-1H-1,2,3-triazole derivatives as tubulin polymerization inhibitors. *Bioorg Chem.* 2019. https://doi.org/10.1016/j.bioorg.2019.103392.
63. Quan YP, Cheng LP, Wang TC, Pang W, Wu FH, Huang JW. Molecular modeling study, synthesis and biological evaluation of Combretastatin A-4 analogues as anticancer agents and tubulin inhibitors. *Medchemcomm.* 2018;9:316–327. https://doi.org/10.1039/c7md00416h.
64. Assali M, Kittana N, Qasem SA, et al. Combretastatin A4-camptothecin micelles as combination therapy for effective anticancer activity. *RSC Adv.* 2019;9:1055–1061. https://doi.org/10.1039/C8RA08794F.
65. Shen YN, Lin L, Qiu HY, Zou WY, Qian Y, Zhu HL. The design, synthesis, in vitro biological evaluation and molecular modeling of novel benzenesulfonate derivatives bearing chalcone moieties as potent anti-microtubulin polymerization agents. *RSC Adv.* 2015;5:23767–23777. https://doi.org/10.1039/c4ra12108b.
66. Gaspari R, Prota AE, Bargsten K, Cavalli A, Steinmetz MO. Structural basis of cis- and trans-combretastatin binding to tubulin. *Chem.* 2017;2:102–113. https://doi.org/10.1016/j.chempr.2016.12.005.
67. Pettit GR, Singh SB, Hamel E, Lin CM, Alberts DS, Garcia-Kendall D. Isolation and structure of the strong cell growth and tubulin inhibitor Combretastatin A-4. *Experientia.* 1989;45:209–211.
68. Pettit GR, Temple C, Narayanan VL, et al. Antineoplastic agents 322. synthesis of Combretastatin A-4 prodrugs. *Anticancer Drug Des.* 1995;10:299–309.
69. Lu Y, Chen J, Xiao M, Li W, Miller DD. An overview of tubulin inhibitors that interact with the colchicine binding site. *Pharm Res.* 2012;29:2943–2971. https://doi.org/10.1007/s11095-012-0828-z.
70. Wang TC, Cheng LP, Huang XY, Zhao L, Pang W. Identification of potential tubulin polymerization inhibitors by 3D-QSAR, molecular docking and molecular dynamics. *RSC Adv.* 2017;7:38479–38489. https://doi.org/10.1039/C7RA04314G.
71. Sriram M, Hall JJ, Grohmann NC, et al. Design, synthesis and biological evaluation of dihydronaphthalene and benzosuberene analogs of the Combretastatins as inhibitors of tubulin polymerization in cancer chemotherapy. *Bioorg Med Chem.* 2008;16:8161–8171. https://doi.org/10.1016/j.bmc.2008.07.050.
72. Wu M, Sun Q, Yang C, et al. Synthesis and activity of Combretastatin A-4 analogues: 1,2,3-thiadiazoles as potent antitumor agents. *Bioorg Med Chem Lett.* 2007;17:869–873. https://doi.org/10.1016/j.bmcl.2006.11.060.
73. Mangiatordi GF, Trisciuzzi D, Alberga D, et al. Novel chemotypes targeting tubulin at the colchicine binding site and unbiasing P-glycoprotein. *Eur J Med Chem.* 2017;139:792–803. https://doi.org/10.1016/j.ejmech.2017.07.037.
74. Mikstacka R, Stefański T, Rózański J. Tubulin-interactive stilbene derivatives as anticancer agents. *Cell Mol Biol Lett.* 2013;18:368–397. https://doi.org/10.2478/s11658-013-0094-z.
75. Kanthou C, Greco O, Stratford A, et al. The tubulin-binding agent Combretastatin A-4-phosphate arrests endothelial cells in mitosis and induces mitotic cell death. *Am J Pathol.* 2004;165:1401–1411. https://doi.org/10.1016/S0002-9440(10)63398-6.
76. Wang LG, Liu XM, Kreis W, Budman DR. The effect of antimicrotubule agents on signal transduction pathways of apoptosis: a review. *Cancer Chemother Pharmacol.* 1999;44:355–361. https://doi.org/10.1007/s002800050989.
77. Zhu M-L, Horbinski CM, Garzotto M, Qian DZ, Beer TM, Kyprianou N. Tubulin-targeting chemotherapy impairs androgen receptor activity in prostate cancer. *Cancer Res.* 2010;70:7992–8002. https://doi.org/10.1158/0008-5472.CAN-10-0585.
78. Mamiya F, Ousaka N, Yashima E. Remote control of the planar chirality in peptide-bound metallomacrocycles and dynamic-to-static planar chirality control triggered by solvent-induced $3_{10}$ -to-α-helix transitions. *Angew Chemie Int Ed.* 2015;54:14442–14446. https://doi.org/10.1002/anie.201507918.
79. Luo Z, Guo Q, Liu X, Ye X, Hongru L, Gao F. Novel two-photon singlet oxygen photosensitizers: experimental and theoretical studies of numbers of bromine atoms effect. *Curr Org Chem.* 2013;17:1–13.
80. Cushman M, Nagarathnam D, Gopal D, Chakraborti AK, Lin CM, Hamel E. Synthesis and evaluation of stilbene and dihydrostilbene derivatives as potential anticancer agents that inhibit tubulin polymerization. *J Med Chem.* 1991;34:2579–2588.
81. Motoshima K, Ishikawa M, Hashimoto Y, Sugita K. Inhibition of restriction enzymes EcoRI, BamHI and HindIII by phenethylphenylphthalimides derived from thalidomide. *Chem Pharm Bull.* 2011;59:880–884. https://doi.org/10.1248/cpb.59.880.
82. Fischer F, Schmutzler F, Haak E. Kondensation von Verbindungen Des Vollacetal-Typs Mit C-H aciden Verbindungen I. Kondensation von Bromacetaldehyddiathylacetal Mit Phenolathern Und von Benzaldehyd-Bisaminalen Des Piperidins Und Morpholins Mit Ketonen. *J Prakt Chemie.* 1964;24:216–225. https://doi.org/10.1002/prac.19640240313.
83. Liu YQ, Li XJ, Zhao CY, et al. Synthesis and insect antifeedant activity of stilbene derivatives against Brontispa Longissima Larvae. *Med Chem Res.* 2013;22:2196–2206. https://doi.org/10.1007/s00044-012-0212-x.